

## Green synthesis of polysaccharides-based gold and silver nanoparticles and their promissory biological activity

Daniela A. Geraldo<sup>1,4\*</sup>, Paula Needham<sup>2</sup>, Nancy Chandia<sup>2</sup>, Ramiro Arratia-Perez<sup>1,4</sup>, Guido C. Mora<sup>3</sup>, Nicolás A. Villagra<sup>3</sup>

<sup>1</sup>Doctorado en Físicoquímica Molecular, Center of Applied Nanosciences (CENAP), Universidad Andres Bello, Ave. Republica 275, Santiago, Chile

<sup>2</sup>Laboratorio de Moléculas Bioactivas, Departamento de Biología Marina, Facultad de Ciencias del Mar, Universidad Católica del Norte, Coquimbo, Chile

<sup>3</sup>Laboratorio de Patogenesis Molecular y Antimicrobianos, Unidad de Microbiología, Facultad de Medicina, Universidad Andres Bello, Santiago, Chile

<sup>4</sup>Núcleo Milenio de Ingeniería Molecular para Catálisis y Biosensores, ICM, Chile

\*corresponding author e-mail address: [daniela.geraldo@unab.cl](mailto:daniela.geraldo@unab.cl)

### ABSTRACT

This paper demonstrates a green approach for the synthesis of gold and silver nanoparticles using polysaccharides extracted from macroseaweed as reducing agents. The formation of Au-NPs and Ag-NPs was confirmed by UV-Vis spectroscopy and Transmission Electron Microscopy (TEM). TEM analysis of both polysaccharides-based metallic nanoparticles surprisingly showed that the type of the polysaccharides (alginate or carrageenan) not only influence the morphology and the sizes of the nanostructures but also avoid the aggregation of them. The biological activity of these eco-friendly metallic nanoparticles was tested on two Gram-negative pathogenic organisms such as *Pseudomonas aeruginosa* and *Salmonella Typhimurium*, showing similar activity than those ones prepared using the well-known inorganic reducing agent, sodium citrate (SC). Furthermore, hemolytic activity was also tested showing that the polysaccharides-based metallic nanoparticles (Ps-MNPs) were less cytotoxic than the corresponding gold and silver nanoparticles prepared using SC. These results strongly suggest that these Ps-MNPs could be used as antimicrobial agents for the treatment of bacterial infections.

### 1. INTRODUCTION

Nanoparticles made by transition metals have been widely synthesized using chemical and physical approaches [1]. However, those elements located in groups IB have gained a lot of attention due to their antimicrobial properties [2-4], optical imaging response for early stage tumor detection as well as, their activity as therapeutic agent for photothermal cancer treatment [5, 6]. Despite this, new approaches to design more safe nanoparticles are required in order to increase its biocompatibility. Bio-assisted synthesis is actually playing an important role due to their clean, non-toxic and environmentally friendly procedures [7]. Biosynthetic methods involving the use of biological organisms have been explored as potential biofactories for synthesis of metallic nanoparticles such as cadmium sulfide, gold, and silver [8-13]. However, the disadvantages of these methods are long time-consuming and require the preparation and maintenance of a cell culture. Alternatively, to these bio-assisted methods, the use of natural reducing agents such as saccharides has gained a lot of attention because they remain inexpensive and also avoid the use of hazardous chemicals decreasing the cytotoxicity of these nanoparticles which benefit their compatibility for biomedical applications. These saccharides have been probed as efficient materials in the preparation of metallic nanoparticles because can be used as reducing and capping agents [14-18]. For example S. Panigrahi et al. [15] have reported a general method for the synthesis of different metal nanoparticles (Au, Ag, Pt, Pd) using commonly available sugars, e.g., glucose, fructose and sucrose as reducing agents where no other stabilizing agent or capping agent

was required to stabilize the nanoparticles. Furthermore, the polymers of monosaccharide (polysaccharides) containing a large number of reactive groups such as hydroxyl, carboxyl and amino groups have been also used to prepared many nanoparticle drug delivery systems [13]. Nevertheless, not much articles have been published about the use of polysaccharides acting as reducing agents for metal salt precursors to produce metallic nanoparticles [19-22]. Referring to polysaccharides of algal origin these include alginates, laminarans and fucans which perform structural functions in marine environment. All of them are abundant in nature; they are important not only as abundant resources, but mainly for their attracting biological properties and potential in the biomedical field. A complete study published by N. Sangeetha et al. [21] reported the use of sodium alginate as template for the synthesis of silver nanoparticle where the stability and the reducing power of this natural polysaccharide was studied under different reaction conditions (concentration, temperature, pH and reaction time). Thus, it was reported that the concentration of both silver nitrate and sodium alginate operated as a controller of nucleation as well as a stabilizer for the nanoparticles. Recently H. M. El-Rafie et al. [19] have also reported the green synthesis of silver nanoparticles using polysaccharides extracted from marine macro algae where the resultant Ag-NPs colloidal solutions were used to modified cotton fabrics for antimicrobial purposes. These results revealed that the antimicrobial activity depends on type of the fabric treatment, size of the synthesized Ag-NPs and the algal species used for polysaccharides extraction. Based on this, in this

work we explored the use of polysaccharides extracted from different seaweed coming from the Chilean coast in order to produce gold and silver nanoparticles. These macroseaweed are ubiquitous in the Chilean coast and their polysaccharides are highly stable, safe, non-toxic, hydrophilic, non-immunogenic and biodegradable. Considering that the most of these natural polysaccharides (alginates, laminarans and fucans) produce

bioadhesion by forming non-covalent bonds with biological tissues (mainly epithelia and mucous membranes) through its hydrophilic groups such as hydroxyl, carboxyl and sulfate groups; we tested the antimicrobial properties and the hemolytic effect of these metallic nanoparticles in comparison with those prepared using the well-known reducing agent, sodium citrate.

## 2. EXPERIMENTAL SECTION

### 2.1 Materials.

Gold (III) chloride trihydrate ( $\geq 99.9\%$  trace metals basis) and sodium citrate dihydrate ( $\geq 99\%$ ) were purchased from Sigma-Aldrich. Silver nitrate (analytical grade) was purchased from Chemix. All aqueous solutions were prepared with Millipore water produced by EasypureII, Thermo scientific. For the disk diffusion assay, we used the following materials: Luria-Bertani Broth, LB (Bactotryptone, 10 g/L; Bacto yeast extract, 5 g/L; and NaCl, 5 g/L); Müeller-Hinton plates (300 g/L beef infusion, 15.5 g/L casein acid hydrolysate, 1.5 g/L starch and 17 g/L agar); PBS buffer (55 mg/mL  $\text{NaH}_2\text{PO}_4 \cdot 7\text{H}_2\text{O}$ , 15 mg/mL  $\text{K}_2\text{HPO}_4$  and 4.25 mg/mL NaCl); Carbonyl Cyanidem-ChloroPhenylhydrazone (CCCP), were purchased from Sigma-Aldrich.

### 2.2 Macro Seaweed.

The red (*Chondracanthuschamissoi*), brown (*LessoniaSpicata*), and green (*Ulvasp*) seaweeds were collected in winter from along the coast of Puerto Aldea, Lagunillas, Punta de Lobos, and La Herradura-Chile. The macroalgal samples were brought to the laboratory in an ice box and cleaned thoroughly with freshwater, the epiphytes were removed. The cleaned macroseaweed were dried in shade at room temperature and well grinded.

### 2.3 Methods.

#### 2.3.1 Extraction and purification of polysaccharides.

Blades of seaweed samples were oven dried at 50 °C for 36 h. The dry seaweed (100 g) was milled (~2 mm size) and stirred for 10 min with 1L petroleum ether (b.p. 40-60 °C). The supernatant was concentrated in vacuum and the extraction process was repeated (10 times) until no more solid residue was obtained from the concentrate. The residual petroleum ether was evaporated at room temperature for 72 h and the algae were treated with 1.6 L of 96% ethanol and 0.4 L of 37% aqueous formaldehyde. After 72 h, the solid was decanted and dried at room temperature. Ground blades pretreated (100 g) of *LessoniaSpicata* was extracted with 3% sodium carbonate solution (2 L) at 50°C for 4 h (BSA1 and BSA2) [23]. Moreover, 100 g of dried algae pretreated of *LessoniaSpicata* were extracted with 500 mL of 2% aqueous calcium chloride solution for 5 h at 85°C (BSF1) [12]. For another hand, 100 g of ground blades pretreated of *LessoniaSpicata* were sequentially extracted with 80% aqueous ethanol at 70°C, 2% aqueous  $\text{CaCl}_2$  at room temperature (BSF2) and 70°C (BSF3), diluted HCl at pH 2.0 (BSF4) and finally with 3% aqueous  $\text{Na}_2\text{CO}_3$  [24]. Algal powder pretreated of *Ulvasp* (100 g) was hydrochloric acid 0.05 M (1% w/v) for 60 min at 85°C (GSU1 and GSU2) [25]. The dried algal material pretreated of *Chondracanthuschamissoi* (100 g) was extracted with

distilled  $\text{H}_2\text{O}$  (2.5 L) at 90°C during 3 h with stirring (RSC1) [26]. After extraction of each algal sample described above has been finished, the mixture was centrifuged (4000 rpm) and supernatant solution was dialyzed against tap water, followed by distilled water, concentrated in vacuum and freeze-dried. The resulting solid was dissolved in 150 mL of distilled water, stirred for 2 h with 1M HCl (50 mL) and centrifuged. The supernatant was neutralized with 1 M NaOH, dialyzed against distilled water, concentrated and freeze-dried.

#### 2.3.2 Total Sugar determination of the polysaccharides extracts.

Total sugar content was determined by phenol-sulfuric acid method [27]. Uronic acid was determined according to method of Filisetti-Cozzi and Carpita [28]. Molecular weight determination by the reducing end assay was performed as described by Park and Johnson [29]. Sulfate content was analyzed by the turbidimetric method of Dogson and Price [30]. D-Galacturonic acid, D-Glucuronic acid, D-Fructose, D-Glucose, D-Galactose, L-Fucose from Sigma-Aldrich Chemical Co., St. Louis, MO, USA were used as standards. Spectra/Por membrane (MWCO 3500) was using for dialysis. The FT-IR spectra of the samples were recorded in a FT-IR Spectrometer model Spectrum Two from Perkin Elmer and the wavenumbers are expressed in  $\text{cm}^{-1}$ .

#### 2.3.3 Synthesis of gold and silver nanoparticles.

0.1 g (or 0.03 g) of each polysaccharide extract was dissolved in 5 mL (or 3 mL) of deionized water at 70 °C. 5  $\mu\text{L}$  of 6 mM  $\text{HAuCl}_4$  solution was added to the phycocolloid suspensions (0.02 g/mL). Moreover, 5  $\mu\text{L}$  of 0.0147 M  $\text{AgNO}_3$  was added to the phycocolloid suspensions (0.01 g/mL). The samples containing the metal salts ions in the polysaccharides extracts were left to react at 70 °C. The reduction of gold and silver ions to the corresponding metallic nanoparticles was routinely monitored by visual inspection of the solution and was confirmed by online absorbance spectra monitoring and TEM.

#### 2.3.4 Antimicrobial susceptibility tests.

The disc diffusion assay we used to determine antibiotic susceptibility to different compounds, was a modification of a standard method described previously [31]. Overnight cultures of tested strains were grown in LB medium. Then, bacteria were washed three times and resuspended in PBS. Aliquots (~ $10^6$  cells) were spread on Müller-Hinton plates and allowed to dry. Holes were made in the agar with using a punch tool and were spotted with 50  $\mu\text{L}$  of different polysaccharides-based nanocompounds (Ps-based Ag NPs and Au NPs). The plates were incubated overnight at 37 °C. The diameters of the zones of growth inhibition were calculated as the average of two

measurements along two axes passing through the center of the inhibition halo. In all cases, diameters differed by no more than 1 mm. Clinical strains used in this study were *Pseudomonas aeruginosa* collected at the Hospital of Pontificia Universidad Católica of Chile and *SalmonellaTyphimurium* (14028s) from other healthcare facilities throughout the country. All bacterial strains were exposed to the same concentration of silver and gold in its different presentations.

As control the corresponding phycocolloid suspension was also tested. Reference nanoparticles of gold and silver, using the

same concentrations of the corresponding precursor solutions, were also synthesized using Turkevich method[32].

### 2.3.5 Determination of hemolysis in blood agar plates.

For the hemolytic assays, 50 uL of gold and silver nanoparticles prepared using RSC1 and BSA1 extracts were spread on blood agar plates. Then, the plates were incubated overnight at 37°C. This assay was carried out using the same concentration of silver and gold in their different presentations. As reference the corresponding phycocolloid suspension was also tested.

## 3. RESULTS SECTION

### 3.1 Characterization of algal polysaccharides.

Chemical analysis data of the purified algal polysaccharides obtained using specific extraction methods for each studied algae are presented in Table 1. The % yield has been calculated based on the dry weight of the alga taken for extraction; other parameters have been presented as the percentage of extracted polysaccharides.

### 3.2 Biosynthesis of metallic nanoparticles.

For the biosynthesis of metallic nanoparticles all those polysaccharides shown in Table 1 were tested as potential reducing agents. While the controls (phycocolloid suspensions) were mostly transparent showing a light yellow color (0.02 g/mL) the formation of gold nanoparticles, after 40 minutes reacting at 70°C, in the presence of 0.03 μmol of H<sub>2</sub>AuCl<sub>4</sub>•3H<sub>2</sub>O was characterized by a violet-purple color suggesting the formation of the nanoparticles (Ps-AuNPs). This change in color is mainly attributed to the characteristic surface Plasmon resonance of gold nanoparticles. By that time of reaction, color changes were only observed for BSA1 and RSC1 extracts, so we realized that only these phycocolloids were able to act as reducing agents in the studied conditions. Moreover, silver nanoparticles were prepared using the same approach describes before. As mentioned above, while the controls (phycocolloid suspensions) were mostly transparent showing a light yellow color, the presence of silver nanoparticles after adding 0.074 μmol of AgNO<sub>3</sub> to each polysaccharides suspensions (0.01 g/mL) was characterized by a pale brown coloration indicating the onset of formation of Ps-Ag NPs. In this case the formation of nanoparticles was observed after 2 h reacting at 70°C. It can be mentioned that this changes in color suggesting the presence of silver nanoparticles, were only observed for BSA1 and RSC1 extracts.

### 3.3 Phycocolloid extracts as natural reducing agent for metal ions precursors.

As was mentioned above gold and silver nanoparticles could be obtained only with those extracts coming from brown and redseaweeds, BSA1 and RSC1, respectively. These polysaccharides extracts containing mainly alginates and carrageenan, see Table 1. Alginate is a structural polysaccharides present in brown seaweeds. Alginate is made up of a linear block copolymer of α-L-guluronic acid and β-D-mannuronic acid[33, 34], see Figure 1. Those blocks vary in size and alternating M and G segments, as well as, random blocks may also be present. This sequential distribution depends on the producing species, and for marine sources, on seasonal and geographical variations.

**Table 1.** Composition of the algal polysaccharides (Ps) from the different macro-seaweeds used in this work. Brown Seaweed Alginate (BSA), Brown Seaweed Fucane (BSF), Green Seaweed Ulvane (GSU) and Red Seaweed Carrageenan (RSC).

Ps	Functional Group	Yield <sup>a</sup> (%)	Carbohydrate	Content <sup>b</sup> (%)				MW <sup>d</sup>
				Sulfate <sup>c</sup>	Uronic acid	Protein		
BSA1	carboxylic	52.1	92.0	nd	100.0	Nd	2,928,101	
BSA2	carboxylic	53.2	92.0	nd	100.0	Nd	52,976	
BSF1	sulfates	3.1	80.6	44.2	14.8	0.4	43,537	
BSF2	sulfates	5.8	92.8	25.3	7.4	0.3	4,296,264	
BSF3	sulfates	6.1	92.4	23.3	9.4	0.2	48,029	
BSF4	sulfates	6.2	79.4	24.9	13.5	0.1	76,961	
GSU1	carboxylic, acetyls, sulfates	16.9	100.0	23.6	10.3	0.3	94,893	
GSU2	carboxylic, acetyls, sulfates	18.5	92.5	17.3	7.2	0.3	9,308,571	
RSC1	sulfates	41.9	51.9	28.0	nd	1.1	88,855	

nd = no detected

<sup>a</sup> % of dried deffatted algae weight

<sup>b</sup> % of sample weight

<sup>c</sup> % of sulfate expressed as SO<sub>3</sub>Na

<sup>d</sup> Molecular weight calculated from the non-reducing end-chain unit

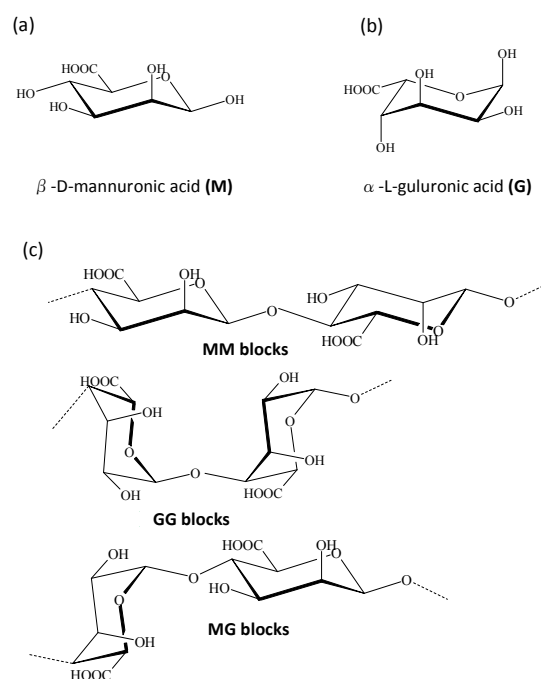


**Figure 1.** Structure of alginic acid extracted from brown seaweed: (a) D-mannuronic residue: M, (b) L-guluronic residue: G and (c) polysaccharide chain: Three different possibilities of residue bonding (MM, GG and MG blocks).

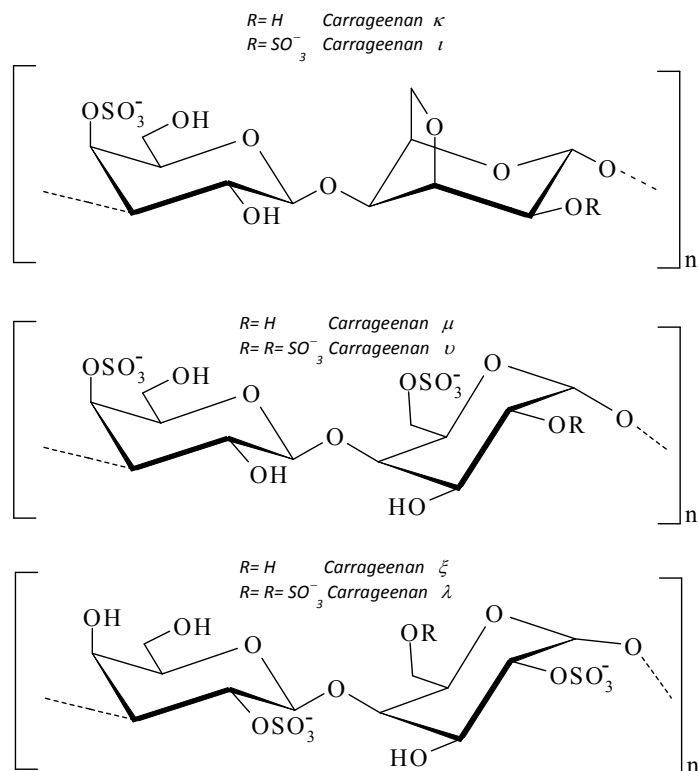


**Figure 2.** Structures of carrageenan family extracted from red seaweed.

Moreover, carrageenans are sulfated polysaccharides that occur as matrix material in several species of red seaweeds and can be extracted with water or aqueous alkali methods [33]. The basic structure of carrageenan is a linear polysaccharide made up of a repeating disaccharide sequence of  $\alpha$ -D-galactopyranose linked 1,3 called the A residue and  $\beta$ -D-galactopyranose residues linked through positions 1,4 (B residues). The number and position of sulfate groups in the repeating galactose units allows the classification of carrageenan in three main commercially relevant families: kappa ( $\kappa$ ), iota ( $\iota$ ) and lambda ( $\lambda$ ) (see Figure 2). It should be stressed that carrageenan can be quite heterogeneous, either due to differing molecular structures within the chains, to differing chains within the seaweed (hybrids) or to algae species, ecophysiology and seasonality or even extraction conditions [33,34]. Indeed, studies suggest that RSC1 extract used in this work are a hybrid of dyads  $\mu$ ,  $\kappa$ , and  $\iota$ .

### 3.4 FT-IR spectroscopy.

As was mentioned above gold and silver nanoparticles could be obtained only with those polysaccharides extracted from brown and red macroseaweed, called RSC1 and BSA1. Figure 3 shows the FT-IR spectra for these two polysaccharides RSC1 and BSA1. These polysaccharides were considered for its structural analysis due to their reducing power against the metal ions precursors of gold and silver. These phycocolloid are characterized for containing sulfated and carboxylic groups, respectively (see Table 1). The FT-IR spectrum Red Seaweed Carrageenan (RSC1) imparts a broad intense band at  $3369\text{ cm}^{-1}$ . These absorption frequencies are assigned to the O-H group of the algal polysaccharides with polymeric association. The band at  $2923\text{ cm}^{-1}$  can be assigned to the alkane C-H stretching vibrations. The absorption band observed at  $1643\text{ cm}^{-1}$  is

attributed to the carbonyl groups of the amide function of proteins present in the algal polysaccharide extracted from *Chondracanthuschamissoi* [35], (see Figure 3a). Specific absorption bands of the fingerprint region for carrageenan are observed at:  $1215\text{ cm}^{-1}$  for the ester sulfate group,  $1067\text{--}1036\text{ cm}^{-1}$  for the S=O stretching vibrations of the sulfated polysaccharides,  $928\text{ cm}^{-1}$  for the 3,6-anhydrogalactose and  $847\text{ cm}^{-1}$  for the galactose-4-sulfate [36]. Moreover, the spectrum for Brown Seaweed Alginate (BSA1) extract, Figure 3b, showed characteristic signals at  $3241$  and  $2925\text{ cm}^{-1}$  which are attributed to the hydroxyl group of alginate forming polymeric association, and to the alkane C-H stretching vibrations in the algal polymer, respectively. Two sharp bands are observed at  $1592$  and  $1408\text{ cm}^{-1}$  representing to asymmetric and symmetric stretching vibrations of carboxylate ion [37], respectively. These bands are in agreement with the high uronic acid content of the product determined by chemical analysis showed in Table 1. The bands at  $1124$ ,  $1084$  and  $1027\text{ cm}^{-1}$  were attributed to the C-O stretching vibration of pyranosyl ring and the C-O stretching with contributions from C-C-H and C-O-H deformation [38]. Spectroscopic analysis by FT-IR for the chosen extracts are in accordance with the chemical composition reported in Table 1.

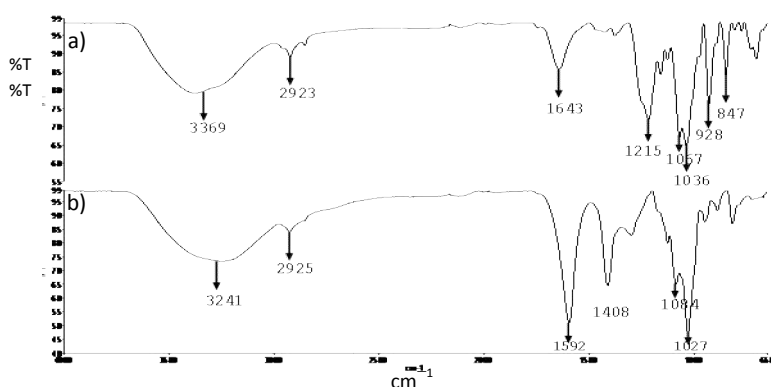


**Figure 3.** FTIR-Transmittance spectra for the polysaccharides extracted from (a) Red Seaweed Carrageenan (RSC1) and (b) Brown Seaweed Alginate (BSA1) corresponding to sulfated and carboxylated polysaccharides, respectively.

### 3.5 Formation of Au nanoparticles (Au NPs).

As mentioned before, the biogenic synthesis of Au NPs took place by addition of an aliquot of the metal salt solution ( $\text{HAuCl}_4$ ) into the phycocolloid suspensions and its further incubation at  $70^\circ\text{C}$  during 40 minutes. The formation of colloidal gold was followed by color change from light yellow to a violet-purple gel-like solution which was checked periodically by UV-Vis spectroscopy. It is observed that only two of the polysaccharides detailed in Table 1 were capable to form gold nanoparticles (BSA1 and RSC1 extracts). According to Table 1, those two extracts contain single functional groups (carboxylates and sulfates) in the polymeric structure respect to the others (see Figure 1 and Figure 2). These results can be attributed to the affinity of alginate and sulfate groups of carrageenan for some divalent and trivalent ions, at acidic pH, which act as crosslinkers between adjacent polymer chains promoting the formation of the biopolymer gels, and the subsequent reduction of gold ions into zero-valent nanoparticles.

Having into account the data shown in Table 1, we hypothesize that the difference on molecular weight between BSA1 and BSA2

extracts should be related to their reducing agent power. Thus, to higher molecular weight greater amount of reducing groups are capable to reduce the metal ions into nanoparticles. Contrarily, those others polysaccharides that contain lower concentrations of uronic acid as well as, a mixture of functional groups (BSF1, BSF2, BSF3, BSF4, GSU1 and GSU2 extracts) were not stronger to reduce gold metal ions into zero-valent nanoparticles.

Based on this, the UV-Vis spectra depicted in Figure 4 shows the presence of the Au surface Plasmon band at 538 and 529 nm for Au-RSC1 and Au-BSA1 nanoparticles, respectively. All the reactions were conducted at room temperature as well as at 70°C in order to determine the effect of the temperature on the polysaccharides-based gold nanoparticles (Ps-Au NPs) formation. Indeed, the formation of Ps-based Au NPs was faster when the reaction was conducted at 70°C instead of at room temperature, data not shown. As described by A. Pal et al.[39] the secondary hydroxyl (–OH) and carboxyl (–COO<sup>–</sup>) functions present in the sodium alginate should be the responsible for the reducing power of this polysaccharide. Thus, the formation of gold nanoparticles would take place subsequently to the chelation of Au (III) by the adjacent hydroxyl functionalities present in the alginate. Alternatively, the synthesis of gold nanoparticles was done using the traditional inorganic reducing agent, sodium citrate in order to compare morphology, aggregation and size distributions between Au@Cit NPs and the polysaccharides-based Au NPs.

From Figure 4 it can be observed that the surface Plasmon resonance wavelength for Au@BSA1 NPs and Au@Cit NPs are very similar (529 nm vs 527 nm), both related with the formation of spherical gold nanoparticles with similar sizes [40]. Furthermore, Au@RSC1 NPs showed two Plasmon bands located at 538 nm and another broad absorption between 650 and 950 nm, in the near-infrared (NIR) region of the electromagnetic spectrum, suggesting the formation of anisotropic particles. This type of anisotropy has been observed when an extract of the plant lemongrass containing aldehydes/ketones was used to reduce chloroaurate ions (AuCl<sub>4</sub><sup>–</sup>) in aqueous solution [41].

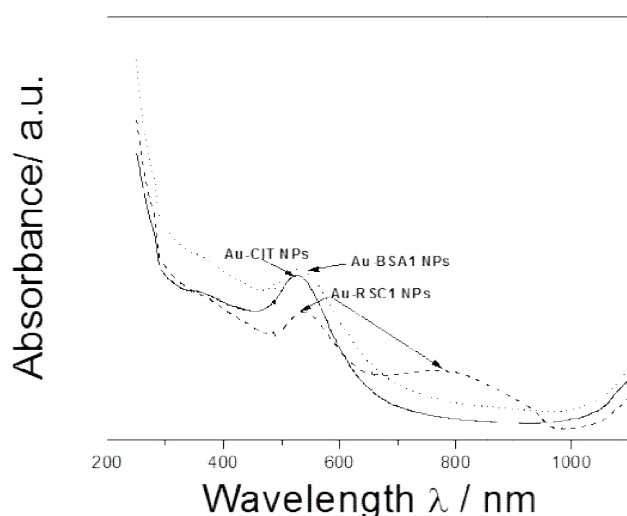


**Figure 4.** UV-Vis spectra of gold nanoparticles synthesized using polysaccharides (Ps) containing sulfates (RSC1) and carboxylic (BSA1) groups as reducing agents. As reference gold-citrate nanoparticles (Au@Cit NPs) were also prepared.

Morphological studies by transmission electron microscopy (TEM) confirmed the presence of anisotropic nanoparticles where both the structure and/or the nature of the polysaccharides may have influenced on the surface properties of the gold nanostructures. Figure 5 depicts the TEM micrographs of gold nanoparticles growing in the presence of **BSA1**, **RSC1** and citrate, respectively. These results obtained from the TEM analysis gives a clear indication regarding the shape and size of the nanoparticles using either phycocolloid or citrate as reducing agents. It can be seen from Figure 5A that the gold nanoparticles formed using **BSA1** phycocolloid suspension were predominantly monodisperse with a uniform size around 25 nm (inset).

Moreover, it can be noted that those Au NPs prepared using this phycocolloid are mostly disaggregated supporting the idea that the polysaccharides extract also acts as stabilizing agent against aggregation. In contrast, TEM images for gold nanoparticles synthesized using sodium citrate (Figure 5C), as reducing agent, showed more polydispersion and aggregation. Furthermore, Figure 5B shows a TEM image of Au NPs synthesized using Red Seaweed Carrageenan (**RSC1**) where surprisingly a mixture of gold nanotriangles showing truncated vertices combined with spherical particles are observed. This is in agreement with those two Plasmon bands in the UV-Vis spectra from Figure 4 where NIR absorption is a consequence of the extended delocalization of the in-plane electrons for the triangular nanoparticles[40].

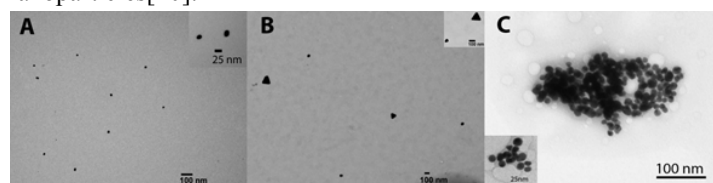


**Figure 5.** TEM micrographs of Gold nanoparticles growing in the presence of: A) BSA1 extract, (B) RSC1 extract and (C) sodium citrate (reference).

### 3.6 Formation of Ag nanoparticles (Ag NPs).

As mentioned above, while the controls (polysaccharides extracts) were mostly transparent showing a light yellow color, the presence of silver nanoparticles after adding an aliquot of AgNO<sub>3</sub> solution to each phycocolloid suspension (0.02 g/ml) was characterized by a pale brown coloration indicating the onset of formation of Ps-Ag NPs. It can be mentioned that this changing in color were only observed for BSA1 and RSC1 extracts. In Figure 6, are depicted the UV-Vis spectra for Ag NPs synthesized using alginate, carrageenan and sodium citrate as reducing agents. It can be seen that the use of alginate (BSA1 extract) induced the formation of silver nanoparticles showing a well-resolved Plasmon peak located at 419 nm (dotted line). According to Kerker (1985), this behavior is related mainly to the presence of spherical single particles with small radii [42]. In contrast, weak and not-well defined Plasmon peaks in the range of 410–440 nm are observed for Ag-RSC1 NPs (dashed line) and Ag@CIT NPs (solid line). These low-resolved peaks have been related to the formation of aggregates that displays optical effects similar to those for prolate spheroids [42]. This is confirmed from Figure 7B where the presence of anisotropic nanoparticles is evident. Based on these results, we propose that the mechanism of formation of silver nanoparticles prepared using sodium alginate is similar to that one

described above for gold nanoparticles [39]. According to S.K. Balabandy et al.[43] after the dispersion of silver ions in the aqueous solution of Na-Alg matrix, Na-Alg reacted with the  $\text{Ag}^+$  to form a Na-Alg complex  $[\text{Ag}(\text{Na-Alg})]^+$ , which further reacts with  $\text{OH}^-$  ions to form Ag-NPs by the reduction of silver ions through the regeneration of alginic acid (Alg) from sodium alginate (Na-Alg). As was mentioned above, we also carried out the synthesis of Ag NPs using sodium citrate in order to compare the effect of green reducing agents (polysaccharides) in the morphology and aggregation of the resulting silver nanoparticles versus to those prepared with SC. It can be noted from Figure 7C that big aggregates are formed in the presence of sodium citrate with a flower-like morphology. However, when alginate is used as reductant less polydisperse nanoparticles exhibiting some grade of isotropy can be obtained (see Figure 7A). Moreover, using carrageenan as reducing agent, Figure 7B, produces anisotropic nanoparticles with highly polydisperse size. It is worth mentioning that this is the first time that the synthesis of gold and silver nanoparticles has been reported using only carrageenan extracted from macroseaweed, as reducing agent. Regarding to the mechanism of formation of the metallic nanoparticles studied in this work, we suggest that gold and silver ions are coordinated by the carrageenan in the same way than the alginate does it with those metal ions[43].

Silver nanoparticles were also analyzed by transmission electron microscopy, thus according to the micrographs showed in Figure 7 we realized that the use of polysaccharides extracts coming from seaweeds as reducing agents not only influence on the nanoparticle sizes but also avoid the aggregation of the final colloids, see Figure 7 (A),(B) and (C).

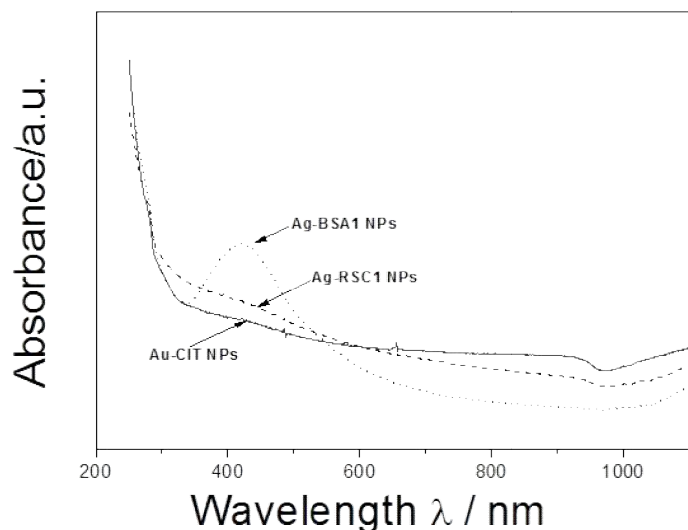


**Figure 6.** UV-Vis spectra of silver nanoparticles synthesized using polysaccharides (Ps) containing sulfates (RSC1) and carboxylic (BSA1) groups as reducing agents. As reference gold-citrate nanoparticles (Au@CIT NPs) were also prepared.

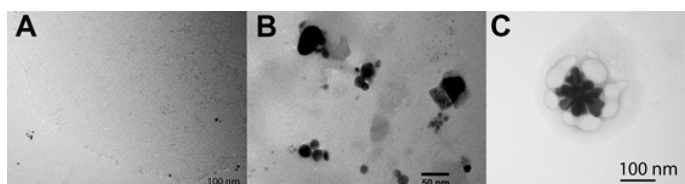


**Figure 7.** TEM micrographs of silver nanoparticles (Ag NPs) prepared using: (A) BSA1 extract and (B) RSC1 extract. Silver nanoparticles synthesized using sodium citrate are used as reference (C).

Figure 7A confirms the formation of predominantly very small silver nanoparticles (lower than 5 nm in size) which are observed as a weak Plasmon peak in the UV-Vis spectrum above. Additionally, bigger particles are also found with ranging size about 10 nm. Finally, TEM images for Ag NPs synthesized using sodium citrate (Figure 7C), show the formation of nanostructures with bigger sizes where citrate was not able to avoid their aggregation. Surprisingly, it can be noted from Figure 7A and 7B that the composition of the polysaccharides (alginates and carrageenan groups) not only did influence in the morphology of the silver nanoparticles, but also determined the size of the final nanoparticles. This interesting phenomenon is under study in our group.

### 3.7 Antimicrobial activity and biocompatibility of polysaccharides-based silver nanoparticles.

The antibacterial activity of pure polysaccharides extracts and polysaccharides-based silver and gold nanoparticles was investigated against two Gram-negative pathogenic organisms such as *Salmonella* Typhimurium (STM 14028s) and *Pseudomonas aeruginosa* (Ps 19422). These pathogens are well known for showing resistance to a wide variety of antibiotics and metal ions[44-47]. The antibacterial efficacy of the polysaccharides-based silver nanoparticles is depicted in Table 2, showing that only RSC1-based Ag NPs were active as antimicrobial agents for *Salmonella* Typhimurium. As expected, Au NPs did not show any activity against these Gram-negative pathogenic organisms under study.

This antimicrobial activity was similar to that one observed using silver ions ( $\text{Ag}^+$ ) as well as silver nanoparticles prepared using citrate, a well-known inorganic reducing agent (Ag@Cit NPs). These results confirmed that phycocolloid coming from red macroseaweed could be used as green reducing agent, where those containing sulfates groups not only produce stable silver nanoparticles but also confer an antimicrobial effect on the resulting metal nanoparticles.

**Table 2.** Antimicrobial activity of pure polysaccharides extracts and polysaccharides-based silver nanoparticles against Gram-negative bacteria. Solutions of  $\text{Ag}^+$  and a suspension of Ag@Cit NPs were used as controls.

Compound	<i>Pseudomonas aeruginosa</i> (Inhibition haloes in mm)	<i>Salmonella Typhimurium</i> (Inhibition haloes in mm)
$\text{Ag}^+$	17	15
Ag@Cit NPs	17	15
BSA1	0	0
Ag@BSA1 NPs	0	0
$\text{Ag}^+$	16	15
Ag@Cit NPs	16	15
RSC1	0	0
Ag@RSC1 NPs	0	13

This activity could be related with the presence of sulfates groups in the polysaccharides which are used in bacteria metabolism and thus, this process would be the responsible of the penetration of Ag NPs inside the bacteria. Furthermore, we suggest that the remarkable differences observed in the antimicrobial effect of the Ag-RSC1 NPs against those two Gram negative bacteria could be related with the differences in the bacterial membrane permeability of these two pathogens. Thus,

although both pathogens use sulfates for their metabolism, the membrane permeability for *Salmonella* (a non-resistant bacterium) that is higher than for *Pseudomonas* (multiresistant bacteria) would make possible the internalization of AgNPs to inside of bacteria [49]. In addition, we must consider the different kind of resistance mechanisms that have both bacteria. *Pseudomonas aeruginosa* have many genes that codifying for resistance to many class of antimicrobial. It is interesting to note that those silver nanoparticles prepared in the presence of polysaccharides containing alginic acid, does not show any antibacterial activity for the bacteria under study which is coherent with the fact that these pathogens does not use carboxylic group in its metabolic pathways. Moreover, according to J.R. Morones et al. [49] silver nanoparticles disturb cell membrane permeability and respiration, and thus once inside the bacteria cause further damage by possibly interacting with sulfur- and phosphorus-containing compounds such as DNA where silver ions releasing will have an additional contribution to the bactericidal effect.

In contrast, Ag-BSA1 NPs exhibited no antimicrobial effect under the tested conditions. Then, we may propose that the antimicrobial effect of polysaccharides based-NPs may be also affected by the molecular weight of the seaweed extract ( $MW_{BSA1}=2,928,101$ ;  $MW_{RSC1}=88,855$ ). So, the higher the molecular weight of polysaccharides, the lower will be the activity of the resulting biogels containing silver nanoparticles. This phenomenon may be rationalized considering that the colloidal size of the Ps-based Ag NPs may be affecting the release of silver ions which are responsible for the antimicrobial effect of Ag NPs [50]. Moreover, as was described by A. E. Nel et al. [51] steric interactions are one of the main forces governing the interfacial interactions between nanomaterials and biological systems. This phenomenon has been observed for polymeric species adsorbed to inorganic particles or biopolymers expressed at the surfaces of cells give rise to spring-like repulsive interactions with other interfaces.

Actually, this condition generally increase stability of individual particles but can interfere in cellular uptake, especially

#### 4. CONCLUSIONS

In this work, gold and silver nanoparticles were successfully synthesized via an easy and eco-friendly one-pot method. The results shown than only polysaccharides such as, sodium alginate (high molecular weight) and carrageenan extracted from brown and red macroseaweed, respectively, were able to act as reducing agents for gold and silver ion solutions but also as stabilizing agent against the aggregation of nanoparticles. Additionally, silver nanoparticles prepared with Brown Seaweed Alginate (BSA) and Red Seaweed Carrageenan (RSC) were tested as antimicrobial agents against *Salmonella Typhimurium* (STM

when surface polymers are highly water-soluble. Finally, in order to evaluate the potential applications of Ps-based silver nanoparticles in nanomedicine, a hemolytic assay using blood agar plates was carried out. As showed in Figure 8, no hemolytic effect was observed on sheep blood cells when silver nanoparticles were prepared using RSC1 and BSA1 extracts (see Figure 8). In contrast, silver nanoparticles prepared using sodium citrate shown hemolytic effect (see white circles) confirming that this reducing agent produces metallic nanoparticles which can induce cytotoxicity in human cells restricting its bioapplications. Indeed, in a previous work has been reported that the presence of sodium citrate residues in gold nanoparticles induced cytotoxicity on human epithelial cells [52], therefore, those results obtained by this new green synthetic approach are highly promissory. Finally, the results obtained in this study support the idea of the potential use Carrageenan-based silver nanoparticles for the treatment of bacterial infections in nanomedicine. Nevertheless, additional studies should be necessary to determine their non-toxic properties on eukaryotes cells.

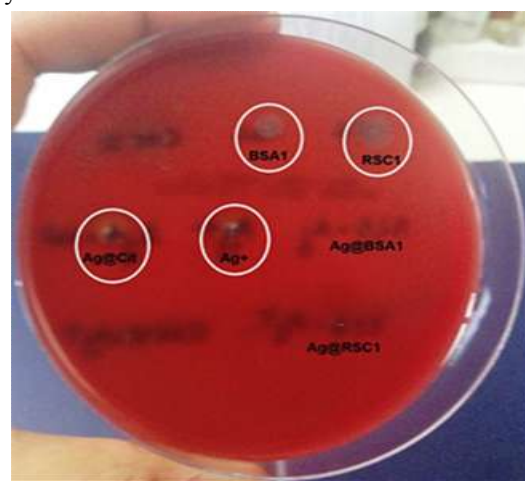


**Figure 8.** Determination of hemolysis induced by polysaccharides-based silver nanoparticles (Ag@BSA1 and Ag@RSC1) on blood agar plate. Ag<sup>+</sup> ions and Ag@Cit NPs were also tested as reference.

14028s) and *Pseudomonas aeruginosa* (Ps 19422). Nevertheless, antimicrobial activity was only observed against *Salmonella Typhimurium* with Ag NPs prepared using Red Seaweed Carrageenan. This phenomenon may be related with the “affinity” of these Gram-negative bacteria for the sulfates groups in the polysaccharide that would make Ag NPs penetration possible. Finally, polysaccharide-based silver nanoparticles synthesized using natural reducing agents showed improved biocompatibility suggesting its potential uses to the treatment of bacterial infections.

#### 5. REFERENCES

- [1] Schmid G., *Nanoparticles: From Theory to Application*, Second, Completely Revised and Updated Edition, Weinheim, WILEY-VCH, **2010**.
- [2] Nowack B., Krug H.F., Height M., 120 Years of Nanosilver History: Implications for Policy Makers, *Environmental Science & Technology*, 45, 4, 1177-1183, **2011**.
- [3] Cioffi N., Torsi L., Ditaranto N., Tantillo G., Ghibelli L., Sabbatini L., Blevè-Zacheo T., D'Alessio M., P., Zambonin P.G., Traversa E., Copper

Nanoparticle/Polymer Composites with Antifungal and Bacteriostatic Properties, *Chemistry of Materials*, 17, 21, 5255-5562, **2005**.

[4] Rai M., Yadav A., Gade A., Silver nanoparticles as a new generation of antimicrobials, *Biotechnology Advances*, 27, 1, 76-83, **2009**.

[5] Ghosh S.K., Pal T., Interparticle coupling effect on the surface plasmon resonance of gold nanoparticles: From theory to applications, *Chemical Reviews*, 107, 11, 4797-4862, **2007**.

- [6] Hu M., Chen J.Y., Li Z.Y., Au L., Hartland G.V., Li X., Marquez M., Xia Y., Gold nanostructures: engineering their plasmonic properties for biomedical applications, *Chemical Society Reviews*, 35, 11, 1084-1094, **2006**.
- [7] Mohanpuria P., Rana N., Yadav S., Biosynthesis of nanoparticles: technological concepts and future applications, *Journal of Nanoparticle Research*, 10, 3, 507-517, **2008**.
- [8] Bao H., Hao N., Yang Y., Zhao D., Biosynthesis of biocompatible cadmium telluride quantum dots using yeast cells, *Nano Research*, 3, 7, 481-489, **2010**.
- [9] Nanda A., Saravanan M., Biosynthesis of silver nanoparticles from *Staphylococcus aureus* and its antimicrobial activity against MRSA and MRSE, *Nanomedicine: Nanotechnology, Biology and Medicine*, 5, 4, 452-456, **2009**.
- [10] Narayanan K.B., Sakthivel N., Biological synthesis of metal nanoparticles by microbes, *Advances in Colloid and Interface Science*, 156, 1-2, 1-13, **2010**.
- [11] Larios-Rodriguez E., Rangel-Ayon C., Castillo S.J., Zavala G., Herrera-Urbina R., Bio-synthesis of gold nanoparticles by human epithelial cells, in vivo, *Nanotechnology*, 22, 35, 1-8, **2011**.
- [12] Chandia N.P., Matsuhira B., Characterization of a fucoidan from *Lessonia vadosa* (Phaeophyta) and its anticoagulant and elicitor properties, *International Journal of Biological Macromolecules*, 42, 3, 235-240, **2008**.
- [13] Liu Z., Jiao Y., Wang Y., Zhou C., Zhang Z., Polysaccharides-based nanoparticles as drug delivery systems, *Advanced Drug Delivery Reviews*, 60, 15, 1650-1662, **2008**.
- [14] Panáček A., Kvítek L., Pucek R., Kolář M., Večeřová R., Pizúrová N., Sharma V.K., Nevěčná T., Zbořil R., Silver Colloid Nanoparticles: Synthesis, Characterization, and Their Antibacterial Activity, *The Journal of Physical Chemistry B*, 110, 33, 16248-16253, **2006**.
- [15] Panigrahi S., Kundu S., Ghosh S., Nath S., Pal T., General method of synthesis for metal nanoparticles, *Journal of Nanoparticle Research*, 6, 4, 411-414, **2004**.
- [16] Filippo E., Serra A., Buccolieri A., Manno D., Green synthesis of silver nanoparticles with sucrose and maltose: Morphological and structural characterization, *Journal of Non-Crystalline Solids*, 356, 6-8, 344-350, **2010**.
- [17] Mehta S.K., Chaudhary S., Gradziński M., Time dependence of nucleation and growth of silver nanoparticles generated by sugar reduction in micellar media, *Journal of Colloid and Interface Science*, 343, 2, 447-453, **2010**.
- [18] Dini L., Panzarini E., Serra A., Buccolieri A., Manno D., Synthesis and in vitro cytotoxicity of glycans-capped silver nanoparticles, *Nanomaterials and Nanotechnology*, 1, 1, 58-63, **2011**.
- [19] El-Rafie H.M., El-Rafie M.H., Zahran M.K., Green synthesis of silver nanoparticles using polysaccharides extracted from marine macroalgae, *Carbohydrate Polymers*, 96, 2, 403-410, **2013**.
- [20] Soisuwan S., Warisnoicharoen W., Lirdprapamongkol K., Svasti J., Eco-friendly synthesis of fucoidan-stabilized gold nanoparticles, *American Journal of Applied Sciences*, 7, 8, 1038-1042, **2010**.
- [21] Sangeetha N., Manikandan S., Singh M., K. Kumaraguru A., Biosynthesis and Characterization of Silver Nanoparticles Using Freshly Extracted Sodium Alginate from the Seaweed *Padina tetrastromatica* of Gulf of Mannar, India, *Current Nanoscience*, 8, 5, 697-702, **2012**.
- [22] Rajeshkumar S., Malarkodi C., Gnanajobitha G., Paulkumar K., Vanaja M., Kannan C., Annadura G., Seaweed-mediated synthesis of gold nanoparticles using *Turbinaria conoides* and its characterization, *Journal of Nanostructure in Chemistry*, 3, 1, 1-7, **2013**.
- [23] Chandia N.P., Matsuhira B., Vásquez A.E., Alginate in *Lessonia trabeculata*: characterization by formic acid hydrolysis and FT-IR spectroscopy, *Carbohydrate Polymers*, 46, 1, 81-87, **2001**.
- [24] Chandia N.P., Matsuhira B., Ortiz J.S., Mansilla A., Carbohydrates from the sequential extraction of *Lessonia vadosa* (Phaeophyta), *Journal of the Chilean Chemical Society*, 50, 2, 501-504, **2005**.
- [25] Robic A., Rondeau-Mouro C., Sassi J.F., Lerat Y., Lahaye M., Structure and interactions of ulvan in the cell wall of the marine green alga *Ulvarotunda* (Ulvales, Chlorophyceae), *Carbohydrate Polymers*, 77, 2, 206-216, **2009**.
- [26] Matsuhira B., Conte A.F., Damonte E.B., Kolender A.A., Matulewicz M.C., Mejías E.G., Pujol C.A., Zúñiga E.A., Structural analysis and antiviral activity of a sulfated galactan from the red seaweed *Schizymeniabinderi* (Gigartinales, Rhodophyta), *Carbohydrate Research*, 340, 15, 2392-2402, **2005**.
- [27] DuBois M., Gilles K.A., Hamilton J.K., Rebers P.A., Smith F., Colorimetric Method for Determination of Sugars and Related Substances, *Analytical Chemistry*, 28, 3, 350-356, **1956**.
- [28] Filisetti-Cozzi T.M.C.C., Carpita N.C., Measurement of uronic acids without interference from neutral sugars, *Analytical Biochemistry*, 197, 1, 157-162, **1991**.
- [29] Park J.T., Johnson M.J., A submicrodetermination of glucose, *Journal of Biological Chemistry*, 181, 1, 149-151, **1949**.
- [30] Dodgson K.S., Price R.G., A note on the determination of the ester sulphate content of sulphated polysaccharides, *Biochemical Journal*, 84, 1, 106-110, **1962**.
- [31] Bauer A.W., Kirby W.M., Sherris J.C., Turck M., Antibiotic susceptibility testing by a standardized single disk method, *American Journal of Clinical Pathology*, 45, 4, 493-496, **1966**.
- [32] Frens G., Controlled Nucleation for the Regulation of the Particle Size in Monodisperse Gold Suspensions. *Nature Physical Science*, 241, 105, 20-22; and references cited therein, **1973**.
- [33] Coviello T., Matricardi P., Marianecchi C., Alhaique F., Polysaccharide hydrogels for modified release formulations, *Journal of Controlled Release*, 119, 1, 5-24, **2007**.
- [34] Silva T.H., Alves A., Popa E.G., Reys L.L., Gomes M.E., Sousa R.A., Silva S.S., Mano J.F., Reis R.L., Marine algae sulfated polysaccharides for tissue engineering and drug delivery approaches, *Biomater*, 2, 4, 278-289, **2012**.
- [35] Kong J., Yu S., Fourier Transform Infrared Spectroscopic Analysis of Protein Secondary Structures, *Acta Biochimica et Biophysica Sinica*, 39, 8, 549-559, **2007**.
- [36] Volery P., Besson R., Schaffer-Lequart C., Characterization of Commercial Carrageenans by Fourier Transform Infrared Spectroscopy Using Single-Reflection Attenuated Total Reflection, *Journal of Agricultural and Food Chemistry*, 52, 25, 7457-7463, **2004**.
- [37] Bi F., Mahmood S.J., Arman M., Taj N., Iqbal S., Physicochemical characterization and ionic studies of sodium alginate from *Sargassum terrarium* (brown algae), *Physics and Chemistry of Liquids*, 45, 4, 453-461, **2007**.
- [38] Daemi H., Barikani M., Synthesis and characterization of calcium alginate nanoparticles, sodium homopolymannuronate salt and its calcium nanoparticles, *Scientia Iranica*, 19, 6, 2023-2028, **2012**.
- [39] Pal A., Esumi K., Pal T., Preparation of nanosized gold particles in a biopolymer using UV photoactivation, *Journal of Colloid and Interface Science*, 288, 2, 396-401, **2005**.
- [40] Tréguer-Delapierre M., Majimel J., Mornet S., Duguet E., Ravaine S., Synthesis of non-spherical gold nanoparticles, *Gold Bulletin*, 41, 2, 195-207, **2008**.



- [41] Shankar S.S., Rai A., Ankamwar B., Singh A., Ahmad A., Sastry M., Biological synthesis of triangular gold nanoprisms, *Nature Materials*, 3, 7, 482-488, **2004**.
- [42] Kerker M., The optics of colloidal silver: something old and something new, *Journal of Colloid and Interface Science*, 105, 2, 297-314, **1985**.
- [43] Balavandy S.K., Shameli K., Abidin Z.Z., Rapid and Green Synthesis of Silver Nanoparticles via Sodium Alginate Media, *International Journal of Electrochemical Science*, 10, 1, 486-497, **2015**.
- [44] Deshpande L.M., Chopade B.A., Plasmid mediated silver resistance in *Acinetobacter baumannii*, *Biomaterials*, 7, 1, 49-56, **1994**.
- [45] Bang S-W., Clark D.S., Keasling J.D., Cadmium, lead, and zinc removal by expression of the thiosulfate reductase gene from *Salmonella typhimurium* in *Escherichia coli*, *Biotechnology Letters*, 22, 16, 1331-1335, **2000**.
- [46] Deredjian A., Colino C., Brothier E., Favre-Bonte S., Courmoyer B., Nazaret S., Antibiotic and metal resistance among hospital and outdoor strains of *Pseudomonas aeruginosa*, *Research in Microbiology*, 162, 7, 689-700, **2011**.
- [47] Geraldo D.A., Arancibia-Miranda N., Villagra N., Mora G., Arratia-Perez R., Synthesis of CdTe QDs/single-walled aluminosilicate nanotubes hybrid compound and their antimicrobial activity on bacteria, *Journal of Nanoparticle Research*, 14, 12, 1-9, **2012**.
- [48] Ruppé É., Woerther P-L, Barbier F., Mechanisms of antimicrobial resistance in Gram-negative bacilli, *Annals of Intensive Care*, 5, 1, 1-15, **2015**.
- [49] Morones J.R., Elechiguerra J.L., Camacho A., Holt K., Kouri J.B., Ramirez J.T., Yacaman M.J., The bactericidal effect of silver nanoparticles, *Nanotechnology*, 16, 10, 2346-2353, **2005**.
- [50] Rhim J.W., Wang L.F., Hong S.I., Preparation and characterization of agar/silver nanoparticles composite films with antimicrobial activity, *Food Hydrocolloids*, 33, 2, 327-335, **2013**.
- [51] Nel A.E., Madler L., Velegol D., Xia T., Hoek E.M.V., Somasundaran P., Klaessig F., Castranova V., Thompson M., Understanding biophysicochemical interactions at the nano-bio interface, *Nature Materials*, 8, 7, 543-557, **2009**.
- [52] Freese C., Uboldi C., Gibson M., Unger R., Weksler B., Romero I., Couraud P-O., Kirkpatrick C.J., Uptake and cytotoxicity of citrate-coated gold nanospheres: Comparative studies on human endothelial and epithelial cells, *Particle and Fibre Toxicology*, 9, 1, 1-11, **2012**.

## 6. ACKNOWLEDGEMENTS

Financial support for this work was provided by the Air Force Office of Scientific Research Project FA9550-12-1-0367. D.A.G thanks Proyecto Núcleo UNAB DI-622-14N and Project RC120001 of the Iniciativa Científica Milenio (ICM) del Ministerio de Economía, Fomento y Turismo del Gobierno de Chile.

© 2016 by the authors. This article is an open access article distributed under the terms and conditions of the Creative Commons Attribution license (<http://creativecommons.org/licenses/by/4.0/>).